The Stability Analysis of Nonlinear Feedback Systems

A stability condition is developed for multivariable, nonlinear feedback systems. The method is based on a modified sector condition and is combined with a polynomial expansion of the nonlinear system to create viable approximations that can be exploited within the sector bound setting. An example demonstrates the utility of the method in defining stable operating regimes for chemical processes.

Tanes Khambanonda
Ahmet Palazoglu
Jose A. Romagnoli
Department of Chemical Engineering
University of California
Davis, CA 95616

Introduction

The development of methods for the analysis of nonlinear feedback systems (Figure 1) has enjoyed limited success in the past due to restrictions and conservativeness associated with computations of operator gains. Several approaches were introduced including: the principal gain (Mees and Rapp, 1977) which employs the condition number; the numerical range (Kouvaritakis and Mossaheb, 1981) which employs the mapping of Eigenloci; and the sector bound (Zames, 1966; Kouvaritakis and Husband, 1982) which uses a graphical interpretation of Popov's criterion. A recent contribution on the computation of nonlinear gains is by Nikolaou and Manousiouthakis (1989) where they define, for the nonlinear operator, the dynamic gain and the dynamic incremental gain over sets. These techniques carry various degrees of conservativeness and restrictions on the classes of nonlinear elements, and/or may require extensive computational effort.

Another school of thought seeks for the globally linearizing transformations for the nonlinear system (Hunt et al., 1983) and has attracted attention from the chemical engineering community (Hoo and Kantor, 1985; Kravaris and Chung, 1987; Calvet and Arkun, 1988) leading to significant contributions in solving nonlinear control problems. This approach looks for exactly linearizing transformations of the nonlinear system after which linear control theory is applied. However, the conditions assuring the existence of such transformations are somewhat restrictive and computations may be nontrivial. Partial linearization method proposed by Krener (1984), on the other hand, introduces transformations that yield an approximation of the nonlinear operator. Alsop and Edgar (1988) applied this method to the control of a heat exchanger.

In this paper, a modified sector condition is introduced in an attempt to reduce or eliminate the problem associated with the existing sector bound approach, paving the way for a viable stability test for nonlinear closed-loop systems. Our strategy also incorporates a polynomial expansion of the nonlinear system to create approximations that can be exploited within the sector bound framework. This approach is not limited to any class of nonlinear operators and furthermore provides the means to predict regions of stability as opposed to other linearization-based approaches that can yield only yes/no-type stability checks.

In the next section, we outline the sector bound approach and establish a graphical stability condition. This is followed by the concept of polynomial expansion for nonlinear systems that helps us express a nonlinear system by its second-order (or higher) approximation and provide the means to effectively apply the stability condition. Finally, a heat-exchanger model is used to demonstrate the methodology.

Sector Bounds and a Stability Condition

Preliminaries

The sector condition was originally introduced by Zames (1966) for scalar systems. It is modified for multivariable applications by Kouvaritakis and Husband (1982), who also incorporated the normal decomposition of the linear operator which tightens the bound on the gain estimation. In this section, we will briefly review some of the results of Kouvaritakis and Husband (1982). This is to present a complete account of the theory and thus prepare the groundwork for our study.

The sector condition is based on the calculation of upper and lower bounds on the gains of operators. From the input-output mapping (Figure 2), one can bound the gains of a nonlinear operator by the slopes of the smallest cone enveloping the mapped area. The slopes represent the maximum and minimum ratios of the output norm to the input norm. When the nonlinear operator contains memory, that is, if it contains dynamic ele-

Correspondence concerning this paper should be addressed to A. Palazoglu.
J.A. Romagnoli is on leave from PLAPIQUI, Argentina.

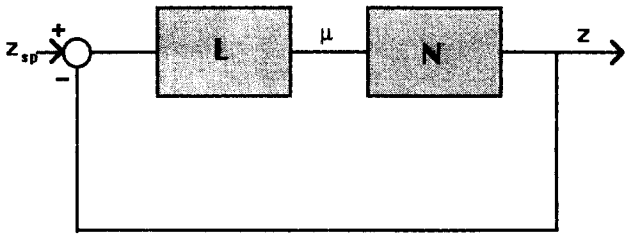

Figure 1. Closed-loop system representation.

ments, the input-output mapping is not unique and this approach cannot be applied.

For linear operators, the sector bound can be conveniently determined in the frequency domain using the Nyquist plots. One can specify the bounds on the operator gains to arrive at an inside sector condition. Moreover, one can also compute the bounds that exclude the operator gains that will lead to an outside sector condition. These conditions will be apparent when we express them mathematically in the following paragraphs. However, before we start reviewing the sector bound concept, it is appropriate to define the function space for the class of problems we are interested in. We assume that the nonlinear operator N is given by:

$$N: L_2^r \rightarrow L_2^r$$

where L_2 denotes the set of Lebesque measurable functions satisfying:

$$f: R \rightarrow R, \quad \text{and} \quad \left[\int_{-\infty}^{\infty} f(x)^2\, dx\right]^{1/2} < \infty$$

Therefore, L_2^r represents the r-dimensional vector-valued class of functions in L_2. The inner product and the L_2^r vector norm are defined in the following fashion:

$$\langle x, y\rangle = \int_{-\infty}^{\infty} x^*(t)y(t)\, dt, \quad \text{and} \quad \|x\| = \langle x, x\rangle^{1/2}$$

Now we can define the sector bounds.

Definition. Let $H: L_2^r \rightarrow L_2^r$, then H is *inside* multivariable sector $[A, B]$, if and only if

$$\langle (H - A)x, (H - B)x\rangle \leq 0, \quad \forall x \in L_2^r \qquad (1)$$

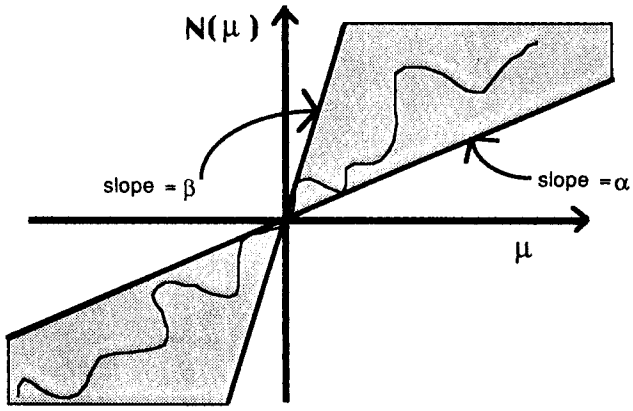

Figure 2. $N(\mu)$ inside sector $[\alpha, \beta]$.

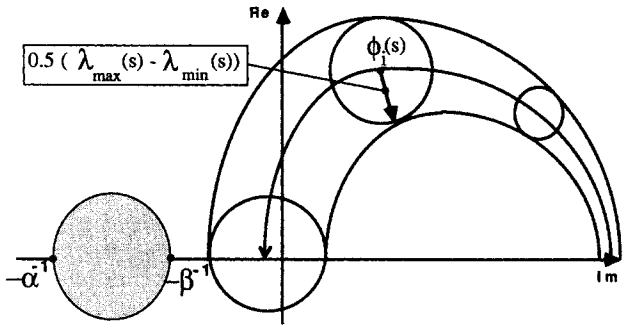

Figure 3. Outside sector condition given by C7.

and *outside* multivariable sector $[A, B]$, if and only if

$$\langle (H - A)x, (H - B)x\rangle \geq 0, \quad \forall x \in L_2^r \qquad (2)$$

Here, we have $A = \text{diag}\ (a_i)$ and $B = \text{diag}\ (b_i)$, where a_i and b_i are real scalars depicting the sector bounds associated with the ith row of H. When $A = aI$ and $B = bI$, and $a < b$, we obtain the scalar sector conditions in place of Eqs. 1 and 2, respectively.

$$\langle (H - aI)x, (H - bI)x\rangle \leq 0, \quad \forall x \in L_2^r \qquad (3)$$

$$\langle (H - aI)x, (H - bI)x\rangle \geq 0, \quad \forall x \in L_2^r \qquad (4)$$

The L_2 vector norm yields an equivalent condition for operators in L_2. For instance, the inside sector condition becomes:

$$\|[H - \tfrac{1}{2}(b + a)I]x\| < \tfrac{1}{2}(b - a)\|x\| \qquad (5)$$

Finally, if the operator H is nonlinear, it is required to satisfy the following conditions:

i. $H(x)$ is nonbiased, $H(0) = 0$,

ii. $H(x)$ is conic positive, $\text{sgn}\ [H_i(x)] = \text{sgn}\ (x_i)$,

iii. $H(x)$ is bounded,

$$\|H(x)\| \leq \text{constant} \cdot \|x\|, \quad \forall x \in X \subset L_2^r$$

iv. $H(x)$ is static (memoryless).

Conditions i–iv may seem at this point to be quite restrictive. However, it will be seen later on that they can be easily satisfied when the sector condition is modified.

Graphical stability condition

The stability criterion for the closed-loop system in Figure 1 can be expressed as:

$$\|L\|_2 \cdot \|N\|_2 < 1 \qquad (6)$$

indicating that the overall loop gain should be less than unity. Here, the operator norm is induced by the two norm for vectors as defined before. Effectively, this condition assures that, if the input z_{sp} is in L_2^r, then the output z will also be in L_2^r, provided that the open-loop system is stable. This can be translated into a sector bound condition by the small-gain Theorem that was originally proposed by Zames (1966) for scalar systems and adopted for multivariable systems by Kouvaritakis and Husband (1982). It is stated that the closed-loop system in Figure 1

is stable if *all* of the following conditions are satisfied and the open-loop system is stable:

C1: L is outside sector $[-\alpha^{-1}, -\beta^{-1}]$, and

C2: N is inside sector $[\alpha, \beta]$.

In order to test the stability condition, we use a graphical interpretation in the frequency domain. Condition C1 analyzes the gain of the linear operator L in order to obtain an estimate on the lower and upper bounds α and β. These values are then substituted into condition C2 to establish the stability condition which the nonlinear operator N must satisfy. The following set of conditions by Kouvaritakis and Husband (1982) is used to test the first condition if L is normal. Here, normal matrices are those with the property $L^*L = LL^*$. It is given that a linear normal operator L has an inside or an outside sector $[\alpha^{-1}, -\beta^{-1}]$ condition, if

C3: The Eigenloci of L are contained *inside* $\mathcal{C}(\alpha^{-1}, \beta^{-1})$, and

C4: The Eigenloci of L are *outside* and do not intersect $\mathcal{C}(-\alpha^{-1}, -\beta^{-1})$.

$\mathcal{C}(\alpha, \beta)$ is the circle with its center on the real axis, passing through points α and β.

To solve for α and β, first the Eigenloci of L are plotted on the complex plane. The largest circle centered on the real axis is then drawn such that the Eigenloci are excluded from the area of the circle. α and β can then be obtained from the circle parameter and the real axis. However, if L is not normal, one can decompose L such that $L = P + \Phi$ where P and Φ are normal matrices. Then we have the following conditions (Kouvaritakis and Husband, 1982) to test C1:

C5: The Eigenvalues of Φ, ϕ_i, do not enter and encircle $\mathcal{C}(-\alpha^{-1} - m, -\beta^{-1} + l)$, for all frequencies ω,

C6: P is inside sector $[l, m]$.

It can be shown that the decomposition of L yields the tightest sector bound when

$$\Phi = (1/2)(L - L^*) + fI \tag{7a}$$

$$P = (1/2)(L + L^*) - fI \tag{7b}$$

where

$$f(s) = (1/2)[\lambda_{\min}(s) + \lambda_{\max}(s)] \tag{8}$$

with $\lambda_{\min}$ and $\lambda_{\max}$ being the minimum and maximum real Eigenvalues of $(1/2)(L + L^*)$ respectively.

If the decomposition is made in accordance with Eq. 3, the eigenvalues of Φ are the sum of the purely imaginary Eigenvalues of $(1/2)(L + L^*)$ and the real Eigenvalues of (fI), i.e.

$$Re(\phi_i) = (1/2)[\lambda_{\min}(s) + \lambda_{\max}(s)] \tag{9}$$

Furthermore, the Eigenvalues of P are real and must lie inside the sector $[(1/2)(\lambda_{\min} - \lambda_{\max}), (1/2)(\lambda_{\max} - \lambda_{\min})]$. This result yields that P is inside $[l, m]$, where

$$l = (1/2)[\lambda_{\min} - \lambda_{\max}] \tag{10a}$$

$$m = (1/2)[\lambda_{\max} - \lambda_{\min}] \tag{10b}$$

To test conditions C5 and C6 with the help of Eq. 7, we establish a graphical procedure. If $L = P + \Phi$, then the feedback system in Figure 1 is stable if *all* of the following conditions are satisfied:

C7: The circle centered at $\phi_i(s)$ with radius $[(1/2)(\lambda_{\max}(s) - \lambda_{\min}(s)]$ does not enter and encircle $\mathcal{C}(-\alpha^{-1}, -\beta^{-1})$, for all s (see Figure 3),

C8: N is inside sector $[\alpha, \beta]$,

The condition C7 represents the sector bound for the *linear* part while C8 is the condition established for the *nonlinear* part. These conditions are dependent on the choice of α and β that are nonunique. The choice which leads to the least conservative stability test is when α is minimum and β is maximum. However, α and β are also interrelated, in the sense that the optimal choice of one also leads to the optimal choice of the other. The following theorem establishes this relationship.

Theorem. The circle centered at $\phi_i(s)$ with radius $[(1/2)(\lambda_{\max}(s) - \lambda_{\min}(s)]$ does not enter and encircle $\mathcal{C}(-\alpha^{-1}, -\beta^{-1})$, for all s, if and only if,

$$\lambda^2_{\max}[1/2(L - L^*)] \le \alpha^{-1}\beta^{-1} + \lambda_{\min}\alpha^{-1} + \lambda_{\max}\beta^{-1} + \lambda_{\min}\lambda_{\max} \tag{11}$$

where $\lambda^2_{\max}[1/2(L - L^*)]$ is given by $\max_{1\le i\le n}\lambda_i^2[1/2(L - L^*)]$.

Proof. See Appendix.

The lefthand side of Eq. 11 is nonpositive since $\lambda_i[0.5(L - L^*)]$ is purely imaginary. Combining this fact with the requirement that $\alpha, \beta > 0$ yields the conclusion that Eq. 11 is satisfied for all α and β if $\lambda_{\min} > 0$, which is essentially a minimum phase condition on the operator. Hence, for that special case, condition C7 is automatically met. And when $\alpha = 0$, this produces a half-plane condition for stability discussed by Mees and Atherton (1980). *In general,* however, the best choice of β is when the inequality in Eq. 11 becomes an equality, i.e., when the two circles just touch each other. The value of β as a function of α can then be found by solving Eq. 11, that yields:

$$\beta = \min_{\omega>0}\left(\frac{\lambda_{\max} + \alpha^{-1}}{\lambda^2_{\max}[1/2(L - L^*)] - \lambda_{\min}\lambda_{\max} - \lambda_{\max}\alpha^{-1}}\right) \tag{12}$$

The importance of this result is that now we can generate the set $\{\alpha, \beta(\alpha)\}$ which will meet the condition on the linear part. The following result enables us to test the stability characteristics of nonlinear closed-loop systems when they satisfy the conditions associated with the sector bound approach.

Result 1. The system in Figure 1 is stable if N is inside sector $[\alpha, \beta(\alpha)]$ where β is defined by Eq. 12. This result is implemented in the context of a robust stability condition and arrives at a stability index in the following section.

Index of stability for nonlinear systems

Here we present a novel method to test the stability of a nonlinear closed-loop system. It has to be understood that the stability condition is deliberately placed within the robustness framework to facilitate the use of approximations to nonlinear systems which will be elaborated in the next section. Consider a linear operator L with an additive-type uncertainty:

$$L' = L + \Delta, \quad \Delta \in \mathbf{\Delta} \tag{13}$$

One can decompose L' into P' and Φ' as in Eq. 7, i.e.

$$\Phi' = \Phi + \delta\Phi \tag{14a}$$

$$P' = P + \delta P \tag{14b}$$

where

$$\delta\Phi = \tfrac{1}{2}(\Delta - \Delta^*) + \tfrac{1}{2}[\delta\lambda_{\min}(s) + \delta\lambda_{\max}(s)] \tag{14c}$$

$$\delta P = \tfrac{1}{2}(\Delta + \Delta^*) - \tfrac{1}{2}[\delta\lambda_{\min}(s) + \delta\lambda_{\max}(s)] \tag{14d}$$

Here $\delta\lambda(s)$ represents the Eigenvalues of $(\frac{1}{2})(\Delta + \Delta^*)$ and P and Φ are defined as in Eq. 7. This decomposition yields the sector bounds on $P'(s)$, i.e., $P'(s)$ is inside sector $[l', m']$ where

$$l' = l + \delta l \tag{15a}$$

$$m' = m + \delta m \tag{15b}$$

and

$$\delta m = -\delta l = \tfrac{1}{2}[\delta\lambda_{\max}(s) - \delta\lambda_{\min}(s)] \tag{15c}$$

In addition, the Eigenloci $\phi_i'(s)$ can be bounded by exploiting a property of normal matrices (Wilkinson, 1966):

$$\|\phi_i'(s) - \phi_i(s)\| < \delta\phi \tag{16}$$

where

$$\delta\phi = \max_{\Delta} \sigma_{\max}(\delta\Phi)$$

Using the results of Eqs. 15 and 16 in conditions C5 and C6, we have the following robust stability criteria.

Result 2. The feedback system in Figure 4 is stable if *all* of the following conditions are satisfied:

C9: The circle centered at $\phi_i(s)$ with radius $\{(\frac{1}{2})[\lambda_{\max}(s) - \lambda_{\min}(s)] + \delta m + \delta\phi\}$ does not enter or encircle $\mathcal{C}(-\alpha^{-1}, -\beta^{-1})$,

C10: N is inside sector $[\alpha, \beta]$,

Parallel to Eq. 11, one can show that the condition C9 is satisfied if and only if,

$$\lambda_{\max}^2(\tfrac{1}{2}(L - L^*)) \le \alpha^{-1}\beta^{-1} + \lambda_{\min}\alpha^{-1} + \lambda_{\max}\beta^{-1} + \lambda_{\min}\lambda_{\max} - \{(\delta\phi + \delta m)^2 + (\delta\phi + \delta m)(\lambda_{\max} - \lambda_{\min} + \alpha^{-1} - \beta^{-1})\} \tag{17}$$

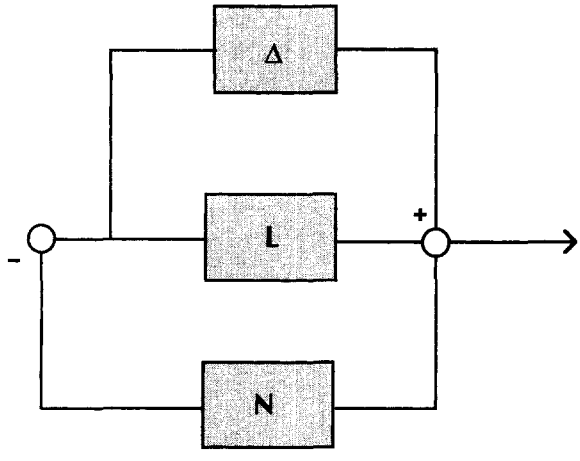

Figure 4. Closed-loop system representation with additive uncertainty.

Hence the best choice of β is:

$$\beta = \min_{\omega>0}\left\{\frac{\lambda_{\max} + \alpha^{-1} + (\delta\phi + \delta m)}{\lambda_{\max}^2[\tfrac{1}{2}(L - L^*)] - \lambda_{\min}\lambda_{\max} - \lambda_{\max}\alpha^{-1} + [(\delta\phi + \delta m)^2 + (\delta\phi + \delta m)(\lambda_{\max} - \lambda_{\min} + \alpha^{-1})]}\right\} \tag{18}$$

With this β, we state the following result:

Result 3. The system in Figure 4 is stable if N is inside sector $[\alpha, \beta(\alpha)]$ with β defined as in Eq. 18.

To test the stability condition in Result 3, Eq. 5 is rephrased as:

$$\|N(x) - \tfrac{1}{2}[\beta(\alpha) + \alpha)Ix]\| < \tfrac{1}{2}(\beta(\alpha) - \alpha)\|x\| \tag{19}$$

For $\alpha < \beta$, one can write,

$$\frac{2\|N(x) - \tfrac{1}{2}[\beta(\alpha) + \alpha]Ix\|}{[\beta(\alpha) - \alpha]\|x\|} < 1 \tag{20}$$

Now we can define the *Index of Stability* for nonlinear feedback systems as:

$$\text{Index}(x) = \max_{\alpha} \frac{2\|N(x) - \tfrac{1}{2}[\beta(\alpha) + \alpha]Ix\|}{[\beta(\alpha) - \alpha]\|x\|}, \quad \forall\alpha < \beta \tag{21}$$

This leads to the main result:

Result 4. The system in Figure 4 is stable at an operating point x, if Index$(x) < 1$.

The Index(x) is unique for a given x, if the nonlinear element is static, that is, it is instantaneous and history-independent. This property of $N(x)$ permits the analysis of Eq. 21, since Index(x) can now be plotted in the state space. Next section will introduce the framework that will enable us to exploit this result.

Nonlinear System Transformation

Let the nonlinear system N_1 be expressed by the following vector equation, where the input enters linearly into the system:

$$\dot{z} = f(z) + g(z)\mu \tag{22}$$

Here, the time argument of the functions is omitted for simplicity. If we expand $f(z)$ and $g(z)$ in homogeneous powers of (z, μ), and define $f^{(2)}$ and $g^{(1)}$ respectively as an n-dimensional vector field and an $n \times n$ matrix whose entries are homogeneous polynomials of degrees 2 and 1 in z, then Eq. 22 can be expressed as:

$$\dot{z} = \Gamma z + \Psi\mu + f^{(2)}(z) + g^{(1)}(z)\mu + (\text{HOT}) \tag{23}$$

Here all the elements of Γ and Ψ as well as of $f^{(2)}$ and $g^{(1)}$ need to be determined. In this polynomial expansion, the vector of higher-order terms (HOT) will be expressed linearly in terms of an uncertain matrix D, where $D = \text{diag}\,(d_1, d_2, \ldots d_n)$,

$$\text{HOT} = Dz \tag{24}$$

The parameter d_i denotes a scalar parameter with uncertainty within the bounds:

$$d_i^l \le d_i \le d_i^u$$

and thus yields the uncertain matrix D. With these results, Eq. 23 reduces to a second-order system with linear uncertainty:

$$\dot{z} = (\Gamma + D)z + \Psi\mu + f^{(2)}(z) + g^{(1)}(z)\mu \qquad (25)$$

Hence the expansion transforms Eq. 22 into a second-order polynomial while still retaining the effect of HOT. It has to be noted that higher-order expansions are also possible and can be used to attenuate the magnitude of the uncertainty. This aspect of our approach will not be discussed here.

Due to the existing degrees of freedom, one can choose d_i to vanish at various steady-state locations within a normal operating region. It is straightforward to see that this happens if and only if

$$f(z_{s,p}) = \Gamma z_{s,p} + f^{(2)}(z_{s,p}) \qquad (26a)$$

$$g(z_{s,p}) = \Psi + g^{(1)}(z_{s,p}) \qquad (26b)$$

where $z_{s,p}$ is the value of the state vector at the pth steady-state point. By the selection of these steady states, one obtains a set of algebraic equations to determine the unknown coefficients of Eq. 23. While these coefficients lead to an exact description of the selected steady states, the general behavior of the system will have to be captured within the uncertainty d_i. We calculate upper and lower bounds on the elements d_i through the following optimization problem:

$$d_i^u = \max_{z\subset Z,\mu\in U} \{[f_i(z) + g_i(z)\mu] - [\Gamma_i^T z + \Psi_i^T\mu + f_i^{(2)}(z) + g_i^{(1)T}(z)\mu]\}\frac{1}{z_i} \qquad (27a)$$

$$d_i^l = \max_{z\subset Z,\mu\in U} \{[f_i(z) + g_i(z)\mu] - [\Gamma_i^T z + \Psi_i^T\mu + f_i^{(2)}(z) + g_i^{(1)T}(z)\mu]\}\frac{1}{z_i} \qquad (27b)$$

Note that the optimization in Eq. 27 is linear with respect to the manipulated variable μ. Furthermore, the range of μ can be limited physically (saturation of control action) or theoretically (violation of physical laws). In addition, since manipulated variables are assumed independent, the optimization of μ simply involves calculation at extreme points of the set U. Similarly, the state variable space Z will also be limited by the normal operating range of the equipment, by acceptable deviations from steady state as imposed by quality control or by the region of safe operation as determined by the operator.

Since most nonlinear elements in process control are history-dependent (dynamic), one must transform (or decompose) the nonlinear operator N_1 into a linear history-dependent part and a nonlinear static residue N, before Eq. 21 can be applied. At this point, we make use of the manipulated variable transformation suggested by Krener (1984) which is of the form:

$$u_j = \mu_j + \tfrac{1}{2}\sum_{k=1}^{n}\sum_{l=1}^{n}\frac{\partial^2 u_j}{\partial z_k \partial z_l}(z^0, \mu^0)x_k x_l + \sum_{k=1}^{n}\sum_{h=1}^{m}\frac{\partial^2 u_j}{\partial z_k \partial \mu_h}(z^0, \mu^0)x_k\mu_h + O(z, \mu)^3 \qquad (28)$$

where $x = z - z^0$, and x and u are the output and input variables of the newly formed linear operator L_2 (Figure 5c). The coefficients of the nonlinear terms in Eq. 28 can be computed in a straightforward manner (see Appendix), taking into account the existing degree of freedom in determining some of these coefficients (Krener, 1984). With this transformation, HOT is eliminated and the transformation becomes exact. Hence, the linear operator L_2 is the first-order linearized form of N_1 (see Figure 5):

$$\dot{x} = Ax + Bu \qquad (29)$$

and A and B matrices are as given in the Appendix.

The linear part is placed in the frequency domain context, utilizing an additive uncertainty:

$$L_1 \cdot L_2 = L + \Delta \qquad (30)$$

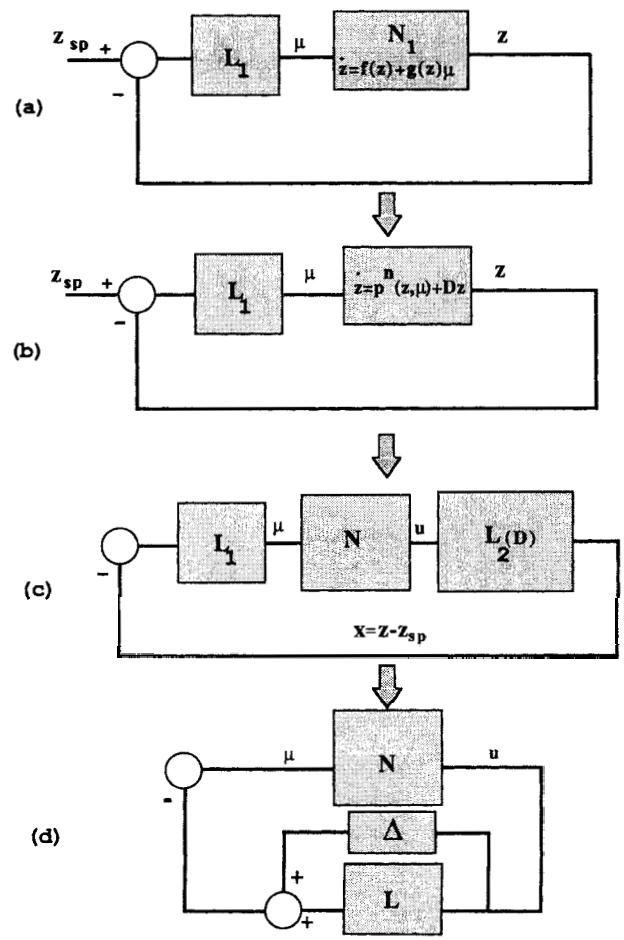

Figure 5. Evolution of the transformations.

Table 1. Model Parameters

$U_h = 198.8$ W/K · m^2	$T_{ca} = 295$ K
$A = 1.9$ m^2	$M_c = 18.15$ kg
$C_{pp} = 1.59$ kJ/kg · K	$C_{pc} = 1.91$ kJ/kg · K
$M_p = 6.8$ kg	$T_{pi} = 366.7$ K
$F_p = 0.19$ kg/s	$F_c = 0.315$ kg/s

with

$$L = [sI - A(d_i = 0)]^{-1}BL_1$$

$$\Delta \in \mathbf{\Delta} = \{\Delta \in C^{n\times m}: \Delta = [(sI - A(d_i))^{-1}BL_1 - L],\ \forall d_i^l \le d_i \le d_i^u\}$$

Now the sector bound for $L + \Delta$ can be calculated as described earlier, and the stability of the closed-loop system can be tested.

The use of manipulated variable transformation along with the polynomial expansion brings about the following advantages:

- Since the first-order approximation is factored out, the resulting nonlinear operator to be bounded is smaller in magnitude than the original nonlinear operator. Now the nonlinear operator is exact due to our expansion, and the uncertainty is lumped to the linear part. This factorization/expansion provides tight stability tests and indeed presents a general framework.
- The polynomial nature of the transformation automatically satisfies the conditions i, ii, iii, regardless of the form of the full nonlinear model they are derived from. Since the transformation is static, this simplifies the computations significantly.
- The evolution of the transformation is displayed in Figure 5. It depicts the path of transformations that we implement to arrive at the final configuration that is now amenable to our stability test.

Example

In this section, a heat-exchanger model that is previously studied by Alsop and Edgar (1989) will be investigated. The nonlinear model is formulated from the energy balance equations:

$$\frac{dT_{co}}{dt} = \frac{2}{M_c}\left[F_c(T_{ci} - T_{co}) - \frac{U_hA_h}{C_{pc}}\Delta T_{lm}\right] \tag{31}$$

$$\frac{dT_{po}}{dt} = \frac{2}{M_p}\left[F_p(T_{pi} - T_{po}) + \frac{U_hA_h}{C_{pp}}\Delta T_{lm}\right] \tag{32}$$

$$\Delta T_{lm} = \frac{[(T_{ci} - T_{po}) - (T_{co} - T_{pi})]}{\ln[(T_{ci} - T_{po})/(T_{co} - T_{pi})]} \tag{33}$$

The heat capacities and the overall heat transfer coefficient are assumed to be constant. The full nonlinear model is linearized to obtain the first-order approximation. The state variables (T_{co}, T_{po}) are also taken as the controlled variables, z_1 and z_2, respectively. The manipulated variables μ_1 and μ_2 are the flow rates, F_c and F_p. These variables are assumed to have a range between zero (fully-closed valve) and the maximum (fully-open valve) as given in Table 1. In standard form, Eqs. 19 and Eq. 20 gives:

$$f(z) = \begin{bmatrix} -\left(\frac{2U_hA_h}{M_cC_{pc}}\right)\Delta T_{lm} \\ \left(\frac{2U_hA_h}{M_pC_{pp}}\right)\Delta T_{lm} \end{bmatrix},$$

$$g(z) = \begin{bmatrix} \frac{2(T_{ci} - T_{co})}{M_c} & 0 \\ 0 & \frac{2(T_{pi} - T_{po})}{M_p} \end{bmatrix} \tag{34}$$

The model equations are expanded according to Eq. 25. The comparison between the model equations and Eq. 25 indicates that some of the coefficients of the second-order expansion is zero, since some of the state and/or manipulated variables do not appear in all of the equations describing the heat exchanger. Hence, Eq. 25 can be rephrased in the following manner:

$$\begin{bmatrix}\dot z_1\\ \dot z_2\end{bmatrix} = \begin{bmatrix}(\gamma_{11} + d_1) & \gamma_{12}\\ \gamma_{21} & (\gamma_{22} + d_2)\end{bmatrix}\begin{bmatrix}z_1\\ z_2\end{bmatrix} + \begin{bmatrix}\zeta_{11} & 0\\ 0 & \zeta_{22}\end{bmatrix}\begin{bmatrix}\mu_1\\ \mu_2\end{bmatrix}$$
$$+ \begin{bmatrix}\Psi_{111} & \Psi_{112} & \Psi_{122}\\ \Psi_{211} & \Psi_{212} & \Psi_{222}\end{bmatrix}\begin{bmatrix}z_1^2\\ z_1z_2\\ z_2^2\end{bmatrix} + \begin{bmatrix}\phi_{111}z_1 & 0\\ 0 & \phi_{222}z_2\end{bmatrix}\begin{bmatrix}\mu_1\\ \mu_2\end{bmatrix}, \tag{35}$$

The operating region within which the system stability characteristics will be tested is chosen such that the maximum temperature variation is within ± 11.1 K of the nominal operating point. This is chosen as the range of state variables used in the computation of Eq. 27. The coefficients γ, ϕ, Ψ, and ζ are computed as described in the previous section and are listed in Table 2. The steady states chosen for the solution of these coefficients are also listed in Table 3. These steady states are believed to sufficiently express the dominant characteristics of the system in the predefined operating region. The process characteristics not captured by these points are described by the uncertainty d_i whose bounds are found by using Eq. 27, and the numerical results are depicted in Table 4.

Table 2. Coefficients of Second-Order Expansion

$\gamma_{11} = 15.79$	$\psi_{111} = -0.0248$	$\zeta_{11} = 0.0325$	$z_1^0 = 317.03$ K
$\gamma_{12} = -15.58$	$\psi_{112} = -0.0002812$	$\zeta_{22} = 0.108$	$z_2^0 = 321.2$ K
$\gamma_{21} = -35.08$	$\psi_{122} = 0.02445$		
$\gamma_{22} = 34.63$	$\psi_{211} = 0.0551$	$\phi_{111} = -1.102 \times 10^{-4}$	$\mu_1^0 = 315$ g/s
	$\psi_{212} = 0.0006248$	$\phi_{222} = -2.94 \times 10^{-4}$	$\mu_2^0 = 189$ g/s
	$\psi_{222} = -0.05434$		

Table 3. Steady-States Selected

No.	$z_1 - z_1^0$	$z_2 - z_2^0$	Comments
1	0	0	Nominal Point
2	11.1	11.1	Extreme Operating Point
3	11.1	−11.1	Extreme Operating Point
4	−11.1	11.1	Extreme Operating Point
5	−11.1	−11.1	Extreme Operating Point

The linear part L_2 (Figure 5c), with the matrices A and B, is expressed as:

$$\dot{x} = \begin{bmatrix} A_{11} + d_1 & A_{12} \\ A_{21} & A_{22} + d_2 \end{bmatrix} \begin{bmatrix} x_1 \\ x_2 \end{bmatrix} + \begin{bmatrix} B_1 & 0 \\ 0 & B_2 \end{bmatrix} \begin{bmatrix} u_1 \\ u_2 \end{bmatrix} \tag{36}$$

The elements of the matrices are defined analytically as follows together with their numerical values for this example:

$$A_{11} = \gamma_{11} + 2\Psi_{111}z_1^0 + \Psi_{112}z_2^0 + \phi_{111}\mu_1^0 = -5.97 \times 10^{-2}$$

$$A_{12} = \gamma_{12} + \Psi_{112}z_1^0 + 2\Psi_{122}z_2^0 = 3.74 \times 10^{-2}$$

$$A_{21} = \gamma_{21} + 2\Psi_{211}z_1^0 + \Psi_{212}z_2^0 = 5.74 \times 10^{-2}$$

$$A_{22} = \gamma_{22} + \Psi_{212}z_1^0 + 2\Psi_{222}z_2^0 + \phi_{222}\mu_2^0 = 0.135$$

$$B_1 = \zeta_{11} + \phi_{111}z_1^0 = -2.49 \times 10^{-3}$$

$$B_2 = \zeta_{22} + \phi_{222}z_2^0 = 1.34 \times 10^{-2}$$

Associated with this, the manipulated variable transformations N (Figure 5c) are also given as:

$$u_1 = \mu_1 + \frac{1}{(\zeta_{11} + \phi_{111}z_1^0)} \cdot [\Psi_{111}x_1^2 + \Psi_{112}x_1x_2 + \Psi_{122}x_2^2 + \phi_{111}x_1\mu_1] \tag{37a}$$

$$u_2 = \mu_2 + \frac{1}{(\zeta_{22} + \phi_{222}z_2^0)} \cdot [\Psi_{211}x_1^2 + \Psi_{212}x_1x_2 + \Psi_{222}x_2^2 + \phi_{222}x_2\mu_2] \tag{37b}$$

For the purpose of demonstrating the calculation of stability bounds, the controller K is assumed to be a simple multiloop proportional controller that has the form:

$$K = k \cdot \begin{bmatrix} 1.2 & 0 \\ 0 & -1.0 \end{bmatrix} \tag{38}$$

where k represents an adjustable gain parameter. The closed-loop system is arranged like the configuration shown in Figure 5d by setting $L_1 = K$ and L_2 as expressed in Eq. 36. Thus, Eq. 30 yields L and Δ. Decomposition of L and Δ is carried out according to Eqs. 13 and 14, followed by the computation of bounds δl, δm, and $\delta\phi$ by Eqs. 15 and 16. Then, β is obtained through the optimization in Eq. 18. β enables us to compute the Index (x) at any point in the state variable space using Eqs. 37 and 21. Note that $x = K^{-1}\mu$ for Eq. 37.

Table 4. Bounds on the Uncertainty

$d_1^l = -0.00985$ $d_1^u = 0.00952$ $d_2^l = -0.0212$ $d_2^u = 0.0219$

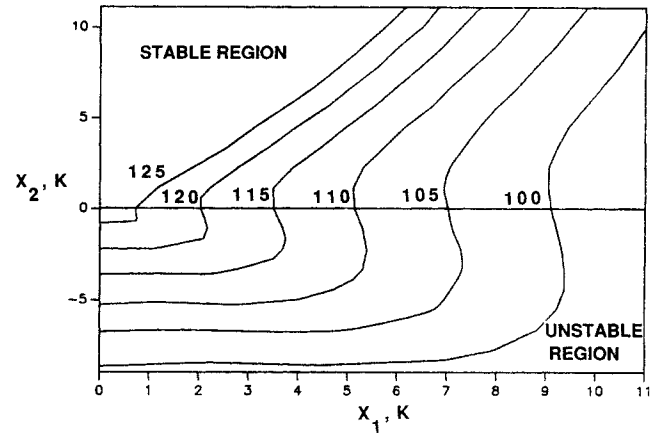

Figure 6. Plot of Index (x_1, x_2) as a function of the controller parameter k.

The Index (x_1, x_2) is computed and the curve along which Index = 1 is plotted in Figure 6 as a function of k. We intend to show how the region of stable operation changes as a function of k. This can be observed by the regions depicted in Figure 6, that continually shrink as the gain is increased. Note that, for high values of k, the stable region will exclude the region ($k > 130$), indicating that the stability of the nominal operating point cannot be guaranteed for those values of k. Therefore, our method indicates that with this controller, such high gains are not permissible for the heat exchanger system. Figure 7 shows the surface associated with the variation of the state variables as a function of k and clearly points out to the diminishing operating range as the gain is increased.

Conclusions

We have developed a stability condition for nonlinear feedback systems that is based on a modified sector condition that optimizes the calculated sector bounds for multivariable operators. With the use of a polynomial expansion for nonlinear operators, one can relax the restrictions on the use of the sector con-

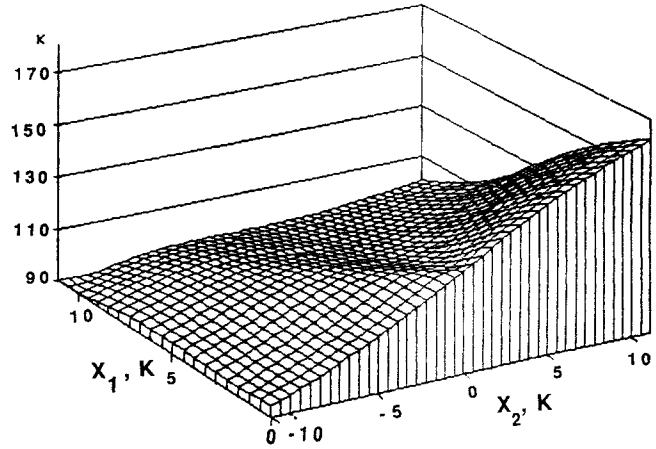

Figure 7. Three-dimensional surface for the Index as a function of the parameter k.

dition for testing the stability of multivariable feedback systems. This resulted in close approximations of nonlinear operator gains and thus convenient tools for stability tests. We have demonstrated the use of the methodology with a heat exchanger example and were able to establish very accurate operating regimes within which the stability of the feedback system is guaranteed.

Notation

A = coefficient matrix in Eq. 29
A_h = heat transfer area
B = coefficient matrix in Eq. 29
C_{pp}, C_{pc} = heat capacities for cold and hot streams
$\mathcal{C}(a, b)$ = circle with its center on the real axis and passing through points a and b
D = diagonal matrix of scalar uncertainty
d_i = scalar uncertainty
F_c, F_p = flow rates of cold and hot streams
H = operator in L_2
I = identity matrix
K = controller matrix
k = controller gain
L = linear operator
L_2 = set of Lebesque measurable functions
L_2^r = r-dimensional vector-valued class of functions in L_2
M_c, M_p = mass flow rate of cold and hot streams
m = dimension of the vector of manipulated variables
N = nonlinear operator
n = dimension of the vector of state variables
P = normal matrix
R = set of real numbers
Re_0 = real part of a complex number
s = Laplace variable
T_c, T_p = temperatures of cold and hot streams
ΔT_{lm} = log-mean temperature difference
U = bounded set of manipulated variables
U_h = overall heat transfer coefficient
u = manipulated variable, linear system
x = state variable, nonlinear system
Z = bounded set of state variables
z = state variable, linear system

Greek letters

Δ = unknown perturbation matrix
$\mathbf{\Delta}$ = set of perturbation matrices
γ = element of matrix Γ
Γ = coefficient matrix in Eq. 23
λ = Eigenvalue of an operator
ϕ_i = ith Eigenvalue of Φ
μ = manipulated variable, nonlinear system
Φ = normal matrix defined by Eq. 7a
σ = singular value
ζ = element of matrix Ψ
Ψ = coefficient matrix in Eq. 23

Subscripts

ci, co = inlet and outlet for cold stream
i, j, k = indices for matrix/vector elements
min = minimum
max = maximum
pi, po = inlet and outlet for hot stream

Superscripts

l = lower bound
T = matrix transpose
u = upper bound
$*$ = complex conjugate transpose
O = steady-state operating point

Literature Cited

Alsop, A. W., and T. F. Edgar, "Nonlinear Heat Exchanger Control Through the Use of Partially Linearized Control Variables," *Chem. Eng. Comm.*, **75,** 155 (1989).

Calvet, J. P., and Y. Arkun, "Feedforward and Feedback Linearization of Nonlinear Systems and Its Implementation Using Internal Model Control," *Ind. Eng. Chem. Res.*, **27,** 1822 (1988).

Hoo, K., and J. Kantor, "An Exothermic Continuous Stirred Tank Reactor is Feedback Equivalent to a Linear System," *Chem. Eng. Comm.*, **37,** 1 (1985).

Hunt, L. R., R. Su, and G. Meyer, "Global Transformations of Nonlinear Systems," *IEEE Trans. on Autom. Contr.* **28,** 24 (1983).

Kouvaritakis, B., and S. Mossaheb, "A Graphical Test of the Small Gain Theorem for Multivariable Nonlinear Systems," *Int. J. Contr.*, **34,** 391 (1981).

Kouvaritakis, B., and R. Husband, "Multivariable Circle Criteria: An Approach Based on Sector Conditions," *Int. J. Contr.*, **35,** 227 (1982).

Kravaris, C., and C. Chung, "Nonlinear State Feedback Synthesis by Global Input-Output Linearization," *AIChE J.*, **33,** 592 (1987).

Krener, A. J., "Approximate Linearization by State Feedback and Coordinate Change," *Sys. & Contr. Lett.*, **5,** 181 (1984).

Mees, A. I., and P. E. Rapp, "Stability Criteria for Multiple loop Nonlinear Feedback Systems," *Proc. IFAC Multivariable Theory*, Pergamon Press (1977).

Mees, A. I., and D. P. Atherton, "The Popov Criterion for Multiloop Feedback Systems," *IEEE Trans. on Autom. Contr.*, **25,** 924 (1980).

Nikolaou, M., and V. Manousiouthakis, "A Hybrid Approach to Nonlinear System Stability and Performance," *AIChE J.*, **35,** 559 (1989).

Wilkinson, J. H., *The Algebraic Eigenvalue Problem*, Clarendon Press, Oxford, England (1966).

Zames, G., "On the Input-Output Stability of Time-Varying Nonlinear Systems: II. Conditions Involving Circles in the Frequency, Plane and Sector Nonlinearities," *IEEE Trans. on Autom. Contr.*, **11,** 228 (1966).

Appendix: Calculation of Manipulated Variable Transformations

With Eq. 25, let's define the following vector functions:

$$F(z) \equiv (\Gamma + D)z + f^{(2)}(z) \tag{A1}$$

$$G(z) \equiv \Psi + g^{(1)}(z) \tag{A2}$$

This leads to the following computations of matrices A and B:

$$A = \frac{\partial F(z^0)}{\partial z} + \frac{\partial G(z^0)}{\partial z} \tag{A3}$$

$$B = G(z^0) \tag{A4}$$

Hence, these matrices are given more explicitly as:

$$A_i = \left[\gamma_{i1} + \sum_{k=1}^{N} \Psi_{i1k} z_k^0 + \sum_{l=1}^{M} \phi_{i11}\mu_1^0 \vdots \cdots\cdots \vdots \gamma_{iN} + \sum_{k=1}^{N} \Psi_{iNk} z_k^0 + \sum_{l=1}^{M} \phi_{iNl}\mu_1^0\right] \tag{A5}$$

$$B_i = \left[\zeta_{i1} + \sum_{k=1}^{N} \phi_{ik1} z_j^0 \vdots \cdots\cdots \vdots \zeta_{iM} + \sum_{k=1}^{N} \phi_{ikM} z_j^0\right] \tag{A6}$$

$$A = \begin{bmatrix} A_1 \\ \cdot \\ \cdot \\ \cdot \\ A_N \end{bmatrix} + D,\ B = \begin{bmatrix} B_1 \\ \cdot \\ \cdot \\ \cdot \\ B_N \end{bmatrix} \tag{A7}$$

with $D = \text{diag}\ (d_1, d_2, \ldots, d_N)$. Here, the coefficients γ, ζ, Ψ, and ϕ are the elements of the matrices Γ, Ψ, $f^{(2)}$ and $g^{(1)}$, respectively. Also the first index i refers to the ith state. We are also indexing the matrices with i to indicate the ith row. The differentiation of the righthand side of Eq. 28 with the help of Eq. 22 reveals the following parameters by comparing the second-order terms in both equations:

$$\sum_{j=1}^{M} G_{ij}(z^0)\, \frac{\partial^2 u_j}{\partial z_k \partial z_l} = \frac{\partial^2 F_i(z)}{\partial z_k \partial z_l} \tag{A8}$$

$$\sum_{l=1}^{N} G_{il}(z^0)\, \frac{\partial^2 u_l}{\partial z_k \partial \mu_j} = \frac{\partial G_{ij}(z)}{\partial z_k} \tag{A9}$$

These are the necessary expressions to compute the coefficients and thus the transformation is complete.

Proof of theorem

Two circles do not intersect if the distance between the two centers is greater than or equal to the sum of their radii. That is,

$$|\phi_i(s) + \tfrac{1}{2}(\alpha^{-1} + \beta^{-1})| \geq \tfrac{1}{2}(\lambda_{\max} - \lambda_{\min}) + \tfrac{1}{2}(\alpha^{-1} - \beta^{-1}) \tag{A10}$$

or,

$$(\lambda_{\min} + \lambda_{\max} + \alpha^{-1} + \beta^{-1})^2 - 4\lambda_i^2[\tfrac{1}{2}(L - L^*)] \geq (\lambda_{\max} - \lambda_{\min} + \alpha^{-1} - \beta^{-1})^2 \tag{A11}$$

The expansion of the terms in Eq. A11 yields,

$$\lambda^2[\tfrac{1}{2}(L - L^*)] \leq \alpha^{-1}\beta^{-1} + \lambda_{\min} + \lambda_{\max}\beta^{-1} + \lambda_{\min}\lambda_{\max} \tag{A12}$$

for all frequencies $\omega > 0$ and for all indices $1 \leq i \leq n$. Q.E.D.

Manuscript received June 6, 1989, and revision received Oct. 17, 1989.